Islamic Azad University

Journal of
Optoelectronical Nanostructures

Winter 2024 / Vol. 9, No. 4

Research Paper

Light absorption and short-circuit current density in plasmonic organic solar cells containing liquid crystal and metal nanowires

M. Soleimani[1], M. J. Karimi *[1], H. Rahimi[2]

[1] Department of Physics, Shiraz University of Technology, Shiraz, Iran
[2] Department of Physics, Yazd University, Yazd, Iran

Received: 18 Aug. 2024
Revised: 20 Oct. 2024
Accepted: 30 Oct. 2024
Published: 15 Nov. 2024

Keywords:
Solar cell
Plasmonic
Organic Material
Absorption

Abstract

In this work, a plasmonic organic solar cell consisting of the organic material P3HT:PCBM, PEDOT:PSS, nematic liquid crystal 5CB, ITO, and metal nanowires was simulated in the wavelength range of 300 to 1200 nm. The substrate and nanowires are made of chrome, copper, and aluminum metals. The refractive indices of the metals were determined from the Drude–Lorentz equation. The values of the geometrical parameters corresponding to the high absorption were calculated. The impact of the layer thicknesses and incident light angle on the short-circuit current density is investigated. The results indicate that the nanowires significantly increase the absorption of the solar cell. Results indicate that the system made of chrome material has a broadband absorption rate of over 90%. Among all the proposed structures, the chrome-based solar cell has a maximum short-circuit current density of approximately $25\,mA/cm^2$. However, this value significantly decreases for incident angles above 40 degrees.

Citation: M. Soleimani, M. J. Karimi, H. Rahimi. Light absorption and short-circuit current density in plasmonic organic solar cells containing liquid crystal and metal nanowires. Journal of Optoelectronical Nanostructures. 2024; 9 (4): 82- 98
DOI: 10.30495/JOPN.2024.33665.1325

Address: Department of Physics, Shiraz University of Technology
Shiraz, 71555-313, Iran. **Tell:** 00987137261392 **Email:** karimi@sutech.ac.ir

1. INTRODUCTION

One type of solar cells (SCs) is organic solar cells (OSCs), characterized by their flexibility, low cost, and lightness. The output current from OSCs depends on the thickness and type of the organic material. Generally, in this category of SCs, the mobility of charge carriers is low. For this reason, the layer of the active material (organic) is relatively thin [1-3].

Over the past decade, numerous studies have been conducted on increasing light absorption and improving the power-conversion efficiency (PCE) of OSCs. One of these methods is the use of nanostructures made of noble (silver, gold) and nonnoble (copper, aluminum, and chrome) metals because of their plasmonic properties [4-6]. The surface plasmon (SP) resonance (SPR) phenomenon occurs on the surface of these nanostructures and increases light trapping [7, 8]. The types of nanostructures used in SCs are nanoparticles (NPs), nanorods (NRs), nanowires (NWs), and nanodiscs (NDs). The geometric parameters of these structures can be controlled; thus, they provide a practical means of increasing the absorption in SCs [7, 9, 10]. Within this context, Baek et al. studied the plasmonic effects of Ag nanoparticles on OSCs [11]. They observed that by adding Ag-NPs, due to the effect of plasmonic scattering, light absorption in the structure increased, and thus the quantum efficiency increased significantly. Ng et al. studied the effect of gold NPs on the electrooptical properties of P3HT:PC70BM layer and SC performance [12]. The effects of Au-NPs on the device optical response were modeled using the FDTD simulation. They observed that the PCE of Au-NPs devices increased remarkably from 7.5% to 8%, 8.1%, and 8.2% for devices with gold NPs, NDs, and nanocubes, respectively. Wang et al. investigated increasing light absorption in the photoactive layer of polymer SCs without raising the thickness of the active layer [13]. They showed that $AuCu_{x-2}S$ nanocrystals enhance the light absorption via local SPR to trap light in the photoactive layer. Xie et al. reported a SP-based structure that improves light absorption in OSCs. They used Ag nanowires in their structure, which can increase light absorption by trapping light in the PEDOT:PSS layer and induce SPs in the P3HT:PCBM absorber layer [14]. These SPs increase the electromagnetic energy around the wires, which improves light absorption. Elrashidi and Elleithy introduced a high-performance OSC based on grating nanostructures in hole and electron transport layers. The grating structure was optimized using the FDTD method. Optical and electrical models were implemented to determine the OSC's performance. They observed that the high absorption in the visible-light region was because the nanogratings [15].

Surface plasmons are sensitive to their surroundings. Their behavior can be manipulated by a nematic liquid crystal (NLC) [16]. NLCs exhibit birefringence, and an electric field can be used to control their optical properties [17]. Another characteristic of NLCs is their ability to enhance the mobility of charge carriers in liquid-crystal devices [18]. Jeong et al. studied the using NLCs of 5CB and C18H19N in OSCs. They found that NLCs increase the absorption in the active layer [19]. They also observed that electron and hole mobilities were enhanced, yielding a PCE of 3.72%, as compared to 2.14% for devices without NLCs. Sun et al. obtained a maximum PCE of 9.3% under AM1.5 solar radiation with a filling factor of 77% by utilizing the NLC characteristics of benzodithiophene terthiophene rhodamine [20].

We recently investigated a plasmonic filter [21] and a thin-film plasmonic solar cell (POSC) composed of NLCs (E7 & E44) [22]. In the present work, we analyze the optical properties of the POSC in the range of 300 -1200 nm. The optical properties were obtained through the finite element method (FEM).

2. STRUCTURE, MATERIALS AND MODELING

A. Structure

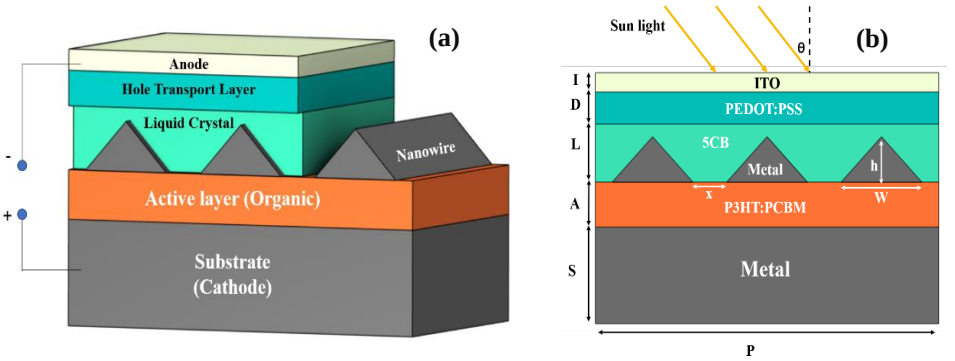

Fig. 1. (a) Three- and (b) two-dimensional schematic diagram of the proposed POSC.

The proposed POSC is illustrated in Fig. 1 and consists of several components: the organic material P3HT:PCBM as the active layer, PEDOT:PSS as the hole transport layer, ITO as the anode, the nematic liquid crystal 5CB, and two metallic layers for the substrate (cathode) and plasmonic nanowires. The metallic components are made of chromium (Cr), copper (Cu), and aluminum (Al). The unit cell geometry is defined by the following parameters: P is the unit cell length; S, A, L, D, and I represent the thicknesses of the substrate, active layer, liquid

crystal layer, hole transport layer, and ITO layer, respectively; w and h denote the width and height of the triangular nanowires; and x is the distance between two nanowires.

B. 2.2 Materials

1) Metals

There are several models such as Drude–Lorentz (DL) and Bernard–Berman models to express the dielectric function of metals, which are generally based on experimental data. In the DL model, the dielectric function is given by [21, 24, 25]:

$$\varepsilon_{DL}(\omega) = 1 - \frac{f_0 \omega_p^{\ 2}}{\omega^2 - i\omega\Gamma_0} + \sum_j \frac{f_i \omega_p^{\ 2}}{\Omega_j^2 - \omega^2 - i\omega\Gamma_j} \quad (1)$$

where ω_p and Ω_j are the plasma and resonance frequencies, f_j and Γ_j are the strength of the oscillators and damping coefficient, respectively. The complex dielectric coefficient is expressed as $\varepsilon(\omega) = (n + ik)^2$ [24, 26]. In Fig. 3a, the refractive indices (n) and extinction coefficients (k) of Cr, Cu and Al are plotted.

2) P3HT: PCBM

One of the materials used in organic bulk-heterojunction SCs as an active material is P3HT:PCBM [27-32]. P3HT and PCBM are employed as electron donor and electron acceptor materials. P3HT:PCBM composition yields an OSC efficiency of around 3% to 5%. These two materials are the most common active layers in OSCs [1, 33, 34].

3) Liquid Crystals

Liquid crystals (LCs) possess characteristics of both liquids and solids; they flow like liquids while maintaining a crystalline molecular structure. These materials exhibit order and mobility across macroscopic, supramolecular, and molecular scales [35]. The dielectric coefficient of the NLCs can be written as follows [36-38]:

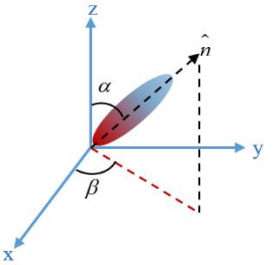

Fig. 2. Schematic of LC molecule.

$$\varepsilon_{xoz} = \begin{bmatrix} n_o^2\cos^2\alpha + n_e^2\sin^2\alpha & 0 & (n_o^2 - n_e^2)\sin\alpha\cos\alpha \\ 0 & n_o^2 & 0 \\ (n_o^2 - n_e^2)\sin\alpha\cos\alpha & 0 & n_o^2\cos^2\alpha + n_e^2\sin^2\alpha \end{bmatrix} \quad (1)$$

$$\varepsilon_{xoy} = \begin{bmatrix} n_e^2\cos^2\beta + n_o^2\sin^2\beta & (n_o^2 - n_e^2)\sin\beta\cos\beta & 0 \\ (n_o^2 - n_e^2)\sin\beta\cos\beta & n_o^2\cos^2\beta + n_e^2\sin^2\beta & 0 \\ 0 & 0 & n_o^2 \end{bmatrix} \quad (2)$$

where α (β) is the angle between $z(x)$ and optical axes (see Fig. 2). Additionally, n_o and n_e denote ordinary and extraordinary refractive indices. For the 5CB NLC (see Fig. 3c), the wavelength (λ) dependence of n_o and n_e is given by [39]:

$$n_o = 1.50849 + 0.00774\lambda^{-2} + 0.00040\lambda^{-4} \quad (3)$$

$$n_e = 1.65535 + 0.01355\lambda^{-2} + 0.00153\lambda^{-4} \quad (4)$$

4) PEDOT:PSS

PEDOT:PSS is usually used as an anodic electrode buffer layer in OSCs. This material acts as a hole transfer layer. In general, the performance of PEDOT:PSS is usually greater than that of ITO and leads to efficient hole extraction [40]. Additionally, the coating a thin layer of PEDOT:PSS can smooth the rough surface of ITO [41, 42].

5) ITO

The anode layer is typically made of ITO or FTO, and must be transparent because it is located behind the active layer [43]. With a band gap of 3.7 eV, ITO largely permits the transmission of photons. Commercial ITO transmits over 80% of visible light.

C. Modeling

One of the numerical methods for solving the wave equation is the FEM. The solution of the FEM is based on dividing large problem into smaller parts called finite elements [44]. The finite element equations are assembled into a comprehensive system to generate the overall representation of the initial problem. The *x*-direction is set with periodic boundary conditions, while perfectly matched layer are implemented in the *y*-direction [45-48].

Maxwell's wave equation is as follows [49, 50]:

$$\nabla \times (\frac{1}{\mu_r} \nabla \times E) - k_0{}^2 (\varepsilon_r - i \frac{\sigma}{\omega \varepsilon_0}) E = 0 \quad (5)$$

where E (electric field), k_0 (free-space wavenumber) and ω (frequency), ε_r (permittivity), μ_r (permeability) and σ (conductivity).

The total absorbed power in the SC with a volume of V is calculated from the following equation [51-54]:

$$A(\lambda) = \frac{1}{2} \int_V \omega |E(x, y, \lambda)|^2 \, \mathrm{Im}[\varepsilon(\lambda)] \, dV \quad (6)$$

One of the important parameters is the solar energy conversion efficiency. The J_{sc} (short-circuit current density) due to the light absorption is calculated by the following integral [53, 55-57]:

$$J_{sc} = \frac{e}{\hbar c} \int_{\lambda_{\min}}^{\lambda_{\max}} A(\lambda) \lambda S(\lambda) \, d\lambda \quad (7)$$

where $S(\lambda)$ is the AM 1.5 solar spectrum, A(λ) is the photon absorption, $\hbar$, e and c are the reduced Plank constant, electron charge, and vacuum speed light.

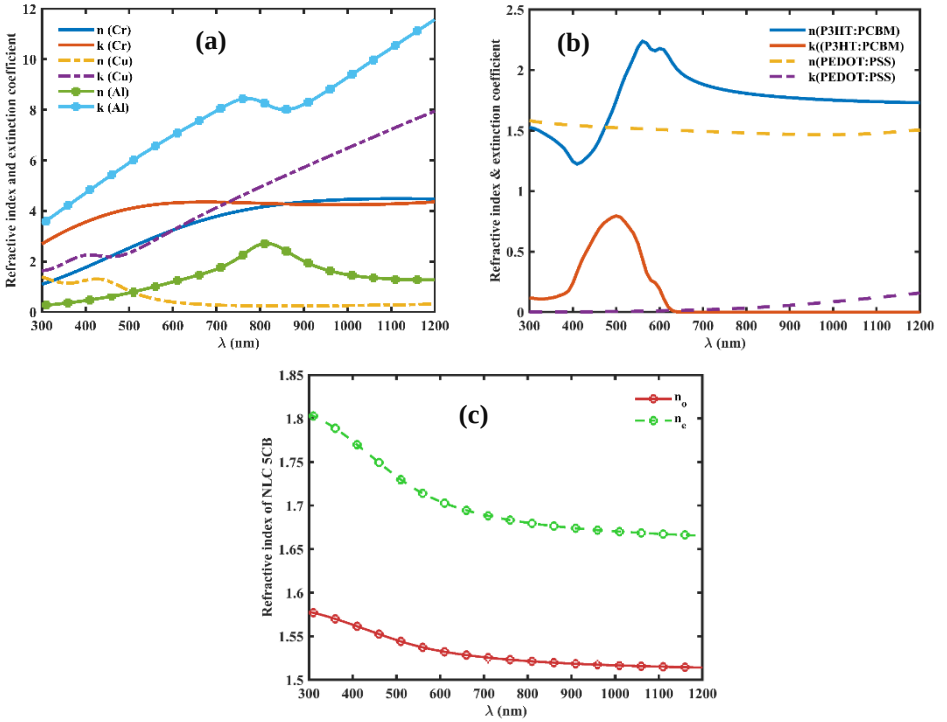

Fig. 3. n and k of the (a) metals [24], (b) P3HT: PCBM, PEDOT:PSS (c) 5CB NLC.

3. RESULTS AND DISCUSSION

The light incident on the SC is AM1.5, with wavelengths ranging from 300 to 1200 nm. Electromagnetic waves radiate uniformly along the z-axis in this structure, with periodic boundary conditions applied on both sides. Additionally, we first consider the angle of sunlight to be zero (perpendicular radiation to the structure) and P=450 nm. Four scenarios for POSC metal parts are examined: both the substrate and nanowires are made of (i) Cr, (ii) Al, (iii) Cu, and (iv) the substrate and nanowires are made of Al and Cr, respectively. Significant absorption is an essential characteristic of efficient SCs. Since the J_{sc} depends on the total absorption of the structure, we calculated the total absorption of the structure (here called absorption). After extensive calculations, we determined the values of the geometry parameters corresponding to the high absorption, which are listed in table 1.

Fig. 4a compares the total absorption of light in the analyzed structures. The Cr and Al-Cr-based POSCs have higher absorption, with an average of more than 90%. In the range of visible light (400 to 700 nm), the Al-Cr structure has a greater

absorption than the Cr-based structure. The Al-based and Cu-based POSCs have absorption intensities lower than 80% in 400-700 nm and 650-950 nm, respectively. Overall, we can conclude that the Cr and Al-Cr structures are more effective than the Cu and Al-based structures. The high and broadband absorption of these structures is attributed to the presence of metal nanowires, as illustrated in Fig. 4b. This figure compares the absorption of Cr-based and Al-Cr-based POSCs with that of structure without nanowires and the data from Ref. [56]. This figure shows that; i) the absorption at wavelengths greater than 600 nm decreases significantly without the presence of nanowires. ii) Although our proposed structure has lower absorption at wavelengths less than 600 nm than the optimized structure of Ref. [56], it has higher absorption at longer wavelengths than the solar cell in this reference.

TABLE I

THE GEOMETRIC SETTING CORRESPONDS TO THE HIGH ABSORPTION OF CR-, AL-, CU-, AND AL-CR-BASED POSC.

Parameters (nm)	Cr	Al	Cu	Al-Cr
A	30	25	80	25
W	110	100	130	120
h	45	25	15	45
L	80	50	90	60
D	30	50	45	30
I	20	20	20	20
S	120	150	150	150

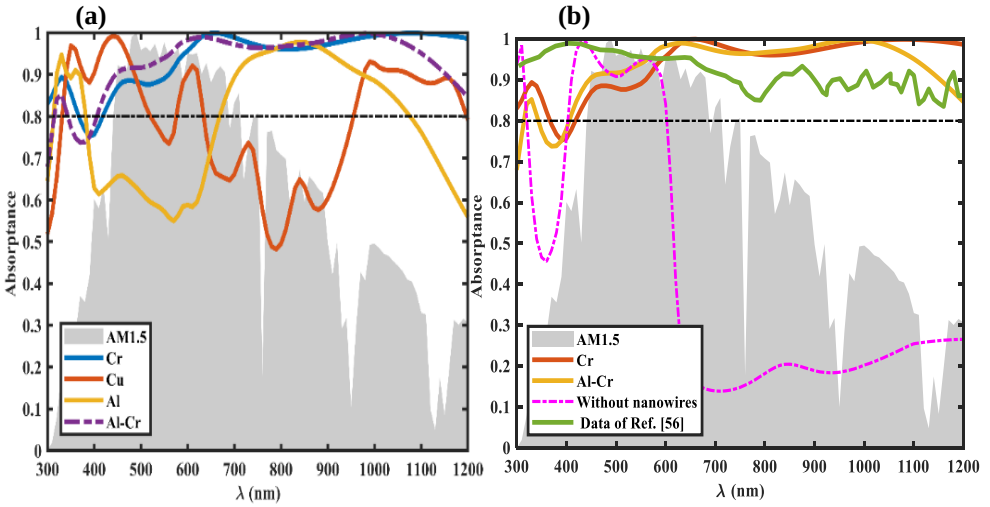

Fig. 4. The total absorption of POSCs with different metal parts: (**a**) Cr, Cu, Al (substrate and nanowires), and Al (substrate)-Cr (nanowires). (**b**) Cr (substrate and nanowires) and Al (substrate)-Cr (nanowires); Comparison with the case without nanowires and the Ref. [56] data.

As mentioned in the introduction, SPR can increase light absorption. Fig. 5 shows the distribution of the electric field norm for the Al-Cr structure at a wavelength of 320 and 650 nm. The absorption increased because the SPR excitations at the interface of the metal and organic layers.

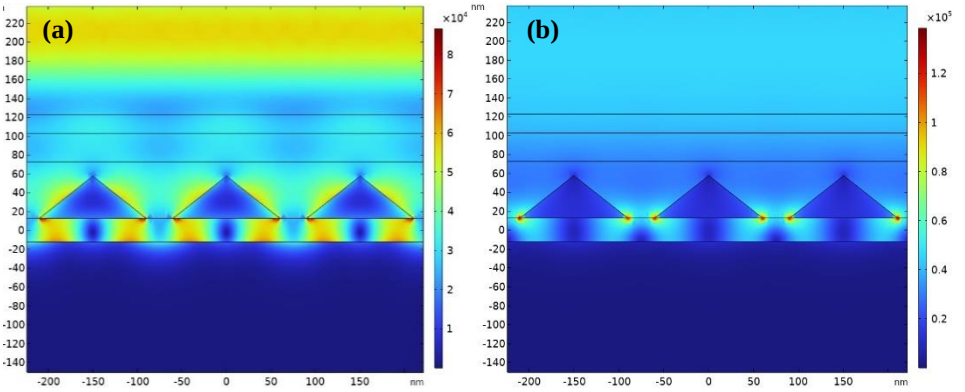

Fig. 5. Electric field (in V/m) norm distribution at: a) $\lambda = 320\,nm$ b) $\lambda = 650\,nm$.

J_{sc} is one of the main important characteristics of SCs. In Fig. 6, the J_{SC} of the Cr-based POSC is plotted versus A, W, and h. This figure shows that J_{SC} increases with these parameters, reaches a maximum, and decreases again. The change in absorption with geometrical parameters is the reason for this behavior. The maximum value of J_{SC} is approximately $24.5\, mA/cm^2$ and occurs when $A = 30.0\, nm$, $W = 110.0\, nm$, and $h = 45.0\, nm$.

In Fig. 7, the variation in J_{SC} with the angle of the light entering the structure is presented. At angles from 0 to 40 degrees, J_{SC} has a small change but decreases meaningfully for angles greater than 40^o. Additionally, the J_{SC} of Cr and Al-Cr POSC is larger than that of Al and Cu-based POSC because of their high absorption.

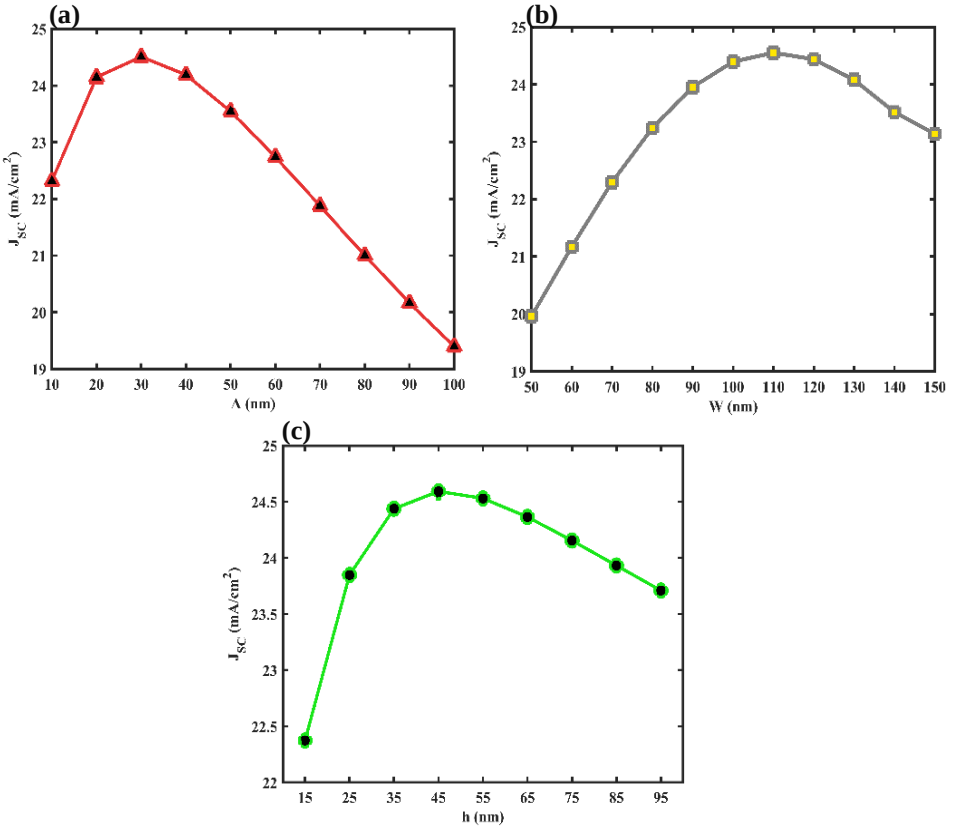

Fig. 6. J_{SC} versus (a) A with $w = 110.0\, nm$ and $h = 45.0\, nm$, (b) w with $A = 30.0\, nm$ and $h = 45.0\, nm$, and (c) h with $A = 30.0\, nm$ and $w = 110.0\, nm$.

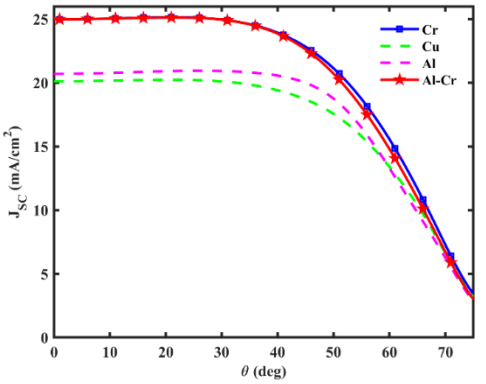

Fig. 7. J_{sc} versus incident light radiation angle (ϴ) for the Cr, Cu, Al, and Al-Cr POSCs.

4. SUMMARY AND CONCLUSION

POSCs, the third generation of SCs, are gaining attention from researchers and industry due to their flexibility and low cost. Utilizing the plasmonic properties of metals can enhance absorption in the active layer of SCs. In the proposed structure, we explored various metals, including Cu, Al, and Cr. The highest absorption was achieved with Cr and Al-Cr configurations. Our findings show that nanowires significantly improve POSC absorption. Since aluminum is commonly used as a substrate and cathode in SCs, an Al-Cr structure is preferable. A key parameter for SCs is the J_{sc} , which varies with geometrical parameters and the angle of incident light. Cr- and Al-Cr-based SCs exhibit a maximum J_{sc} of about 25 mA/cm². Overall, these results could help in the design of POSCs.

5. REFERENCES

[1] G. Li, V. Shrotriya, J. Huang, Y. Yao, T. Moriarty, K. Emery, Y.J.N.m. Yang. *High-efficiency solution processable polymer photovoltaic cells by self-organization of polymer blends*. Nature Mat. 4 (11) (2005) 864-868. Available: https://doi.org/10.1038/nmat1500.

[2] A. Mahmoudloo, Investigation and simulation of recombination models in virtual organic solar cell. Journal of Optoelectronical Nanostructures, 7(4) (2022), 1-12. Available: https://jopn.marvdasht.iau.ir/article_5674.html.

[3] J. Miao, Y. Wang, J. Liu, L.J.C.S.R. Wang. *Organoboron molecules and polymers for organic solar cell applications*. Chem. Soc. Rev. 51 (1) (2022) 153-187. Available: https://doi.org/10.1039/d1cs00974e.

[4] H.I. Park, S. Lee, J.M. Lee, S.A. Nam, T. Jeon, S.W. Han, S.O. Kim. *High Performance Organic Photovoltaics with Plasmonic-Coupled Metal Nanoparticle Clusters*. ACS Nano. 8 (10) (2014) 10305-10312. Available: https://doi.org/10.1021/nn503508p.

[5] D.H. Wang, D.Y. Kim, K.W. Choi, J.H. Seo, S.H. Im, J.H. Park, O.O. Park, A.J.J.A.C. Heeger. *Enhancement of donor–acceptor polymer bulk heterojunction solar cell power conversion efficiencies by addition of Au nanoparticles*. RSC Adv. 123 (24) (2011) 5633-5637. Available: https://doi.org/10.1038/srep01726.

[6] W. Shen, J. Tang, R. Yang, H. Cong, X. Bao, Y. Wang, X. Wang, Z. Huang, J. Liu, L. Huang, J. Jiao, Q. Xu, W. Chen, L.A. Belfiore. *Enhanced efficiency of polymer solar cells by incorporated Ag–SiO2 core–shell nanoparticles in the active layer*. RSC Adv. 4 (9) (2014) 4379-4386. Available: https://doi.org/10.1039/C3RA45495A.

[7] Z. Yuan, Y. Yang, Z. Wu, S. Bai, W. Xu, T. Song, X. Gao, F. Gao, B. Sun. *Approximately 800-nm-Thick Pinhole-Free Perovskite Films via Facile Solvent Retarding Process for Efficient Planar Solar Cells*. ACS Appl Mater Interfaces. 8 (50) (2016) 34446-34454. Available: https://doi.org/10.1021/acsami.6b12637.

[8] M.J. Maleki, M. Soroosh. *A low-loss subwavelength plasmonic waveguide for surface plasmon polariton transmission in optical circuits*. Opt. Quantum Electron. 55 (14) (2023) 1266. Available: https://doi.org/10.1007/s11082-023-05603-0.

[9] K. N'Konou, L. Peres, P. Torchio. *Optical Absorption Modeling of Plasmonic Organic Solar Cells Embedding Silica-Coated Silver Nanospheres*. Plasmonics. 13 (1) (2018) 297-303. Available: https://doi.org/10.1007/s11468-017-0514-4.

[10] D.T. Gangadharan, Z. Xu, Y. Liu, R. Izquierdo, D. Ma. *Recent advancements in plasmon-enhanced promising third-generation solar cells*. J. Nanophotonics. 6 (1) (2017) 153-175. Available: https://doi.org/10.1515/nanoph-2016-0111.

[11] S.-W. Baek, J. Noh, C.-H. Lee, B. Kim, M.-K. Seo, J.-Y. Lee. *Plasmonic Forward Scattering Effect in Organic Solar Cells: A Powerful Optical*

Engineering Method. RSC Adv. 3 (1) (2013) 1726. Available: https://doi.org/10.1038/srep01726.

[12] A. Ng, W.K. Yiu, Y. Foo, Q. Shen, A. Bejaoui, Y. Zhao, H.C. Gokkaya, A.B. Djurišić, J.A. Zapien, W.K. Chan, C. Surya. *Enhanced Performance of PTB7:PC71BM Solar Cells via Different Morphologies of Gold Nanoparticles*. ACS Appl Mater Interfaces. 6 (23) (2014) 20676-20684. Available: https://doi.org/10.1021/am504250w.

[13] H. Wang, Y. Ding, W. Chen, Y. Liu, D. Tang, G. Cui, W. Li, J. Shi, Z. Bo. *Broadband Absorption Enhancement in Polymer Solar Cells Using Highly Efficient Plasmonic Heterostructured Nanocrystals*. ACS Appl Mater Interfaces. 10 (37) (2018) 30919-30924. Available: https://doi.org/10.1021/acsami.8b09101.

[14] R. Xie, Z. Li, E. Gu, S. Guo, Y. Yuan. *Absorption Efficiency Enhancement of Organic Solar Cells by Double Grating Structure*. Photonics Nanostruct. 38 (2020) 100763. Available: https://doi.org/10.1016/j.photonics.2019.100763.

[15] A. Elrashidi, K. Elleithy. *High Performance Polymer Solar Cells Using Grating Nanostructure and Plasmonic Nanoparticles*. Polymers. 14 (5) (2022) 862. Available: https://doi.org/10.3390/polym14050862.

[16] G. Si, Y. Zhao, E.S.P. Leong, Y.J. Liu. *Liquid-Crystal-Enabled Active Plasmonics: A Review*. J. Mater. 7 (2) (2014) 1296-1317. Available: https://doi.org/10.3390/ma7021296.

[17] Y. Sun, L. Jiang, L. Zhong, Y. Jiang, X. Chen. *Towards active plasmonic response devices*. Nano Res. 8 (2) (2015) 406-417. Available: https://doi.org/10.1007/s12274-014-0682-x.

[18] N. Yilmaz Canli, S. Günes, A. Pivrikas, A. Fuchsbauer, D. Sinwel, N.S. Sariciftci, Ö. Yasa, B. Bilgin-Eran. *Chiral (S)-5-octyloxy-2-[{4-(2-methylbuthoxy)-phenylimino}-methyl]-phenol liquid crystalline compound as additive into polymer solar cells*. Sol. Energy Mater. 94 (6) (2010) 1089-1099. Available: https://doi.org/10.1016/j.solmat.2010.02.030.

[19] S. Jeong, Y. Kwon, B.D. Choi, G. Kwak, Y.S.J.M.c. Han, physics. *Effects of nematic liquid crystal additives on the performance of polymer solar cells*. Macromol. Chem. Phys. 211 (23) (2010) 2474-2479. Available: https://doi.org/10.1002/macp.201000379.

[20] K. Sun, Z. Xiao, S. Lu, W. Zajaczkowski, W. Pisula, E. Hanssen, J.M. White, R.M. Williamson, J. Subbiah, J. Ouyang, A.B. Holmes, W.W.H. Wong, D.J.

Jones. *A molecular nematic liquid crystalline material for high-performance organic photovoltaics*. Nat. Commun. 6 (1) (2015) 6013. Available: https://doi.org/10.1038/ncomms7013.

[21] H. Rahimi, M.J. Karimi. *Optical absorption of a metal–liquid crystal–metal plasmonic filter*. Opt. Commun. 485 (2021) 126735. Available: https://doi.org/10.1016/j.optcom.2020.126735.

[22] H. Rahimi, M.J. Karimi, S. Ghajarpour-Nobandegani. *Chromium nanostructures for enhancing light trapping in a thin-film solar cell*. Opt. Mater. 121 (2021) 111548. Available: https://doi.org/10.1016/j.optmat.2021.111548.

[23] S.N. Jafari, A. Ghadimi, S. Rouhi. *Strained Carbon Nanotube (SCNT) thin layer effect on GaAs solar cells efficiency*. Journal of Optoelectronical Nanostructures. 5 (4) (2020) 87-110. Available: https://jopn.marvdasht.iau.ir/article_4505.html.

[24] A.D. Rakić, A.B. Djurišić, J.M. Elazar, M.L. Majewski. *Optical properties of metallic films for vertical-cavity optoelectronic devices*. Appl. Opt. 37 (22) (1998) 5271-5283. Available: https://doi.org/10.1364/AO.37.005271.

[25] A. Abdolahzadeh Ziabari, S. Royanian, R. Yousefi, S. Ghoreishi. *Performance improvement of ultrathin CIGS solar cells using Al plasmonic nanoparticles: The effect of the position of nanoparticles*. Journal of Optoelectronical Nanostructures. 5 (4) (2020) 17-32. Available: https://jopn.marvdasht.iau.ir/article_4506.html

[26] S. Magdi, D. Ji, Q. Gan, M.A. Swillam. *Broadband absorption enhancement in organic solar cells using refractory plasmonic ceramics*. J. Photonics Energy. 11 (1) (2017) 016001.

[27] J. Burschka, N. Pellet, S.-J. Moon, R. Humphry-Baker, P. Gao, M.K. Nazeeruddin, M. Grätzel. *Sequential deposition as a route to high-performance perovskite-sensitized solar cells*. Nature. 499 (7458) (2013) 316-319. Available: https://doi.org/10.1038/nature12340.

[28] M. Liu, M.B. Johnston, H.J. Snaith. *Efficient planar heterojunction perovskite solar cells by vapour deposition*. Nature. 501 (7467) (2013) 395-398. Available: https://doi.org/10.1038/nature12509.

[29] J. Oh, H.-C. Yuan, H.M. Branz. *An 18.2%-efficient black-silicon solar cell achieved through control of carrier recombination in nanostructures*. Nat. Nanotechnol. 7 (11) (2012) 743-748. Available: https://doi.org/10.1038/nnano.2012.166.

[30] F. Zhang, X. Han, S.-t. Lee, B.J.J.o.M.C. Sun. *Heterojunction with organic thin layer for three dimensional high performance hybrid solar cells*. J. Mater. Chem. 22 (12) (2012) 5362-5368. Available: https://doi.org/10.1039/C2JM15674A.

[31] Y. Zhu, T. Song, F. Zhang, S.-T. Lee, B. Sun. *Efficient organic-inorganic hybrid Schottky solar cell: The role of built-in potential*. Appl. Phys. Lett. 102 (11) (2013) Available: https://doi.org/10.1063/1.4796112.

[32] A. Mahmoudloo. *Investigation and Simulation of Recombination Models in Virtual Organic Solar Cell*. Journal of Optoelectronical Nanostructures. 7 (4) (2022) 1-12.

[33] K.A. Emery. *Roles of donor and acceptor nanodomains in 6% efficient thermally annealed polymer photovoltaics*. Appl. Phys. Lett. 91 (26) (2007) Available: https://doi.org/10.1063/1.2817240.

[34] L.M. Chen, Z. Hong, G. Li, Y. Yang. *Recent Progress in Polymer Solar Cells: Manipulation of Polymer:Fullerene Morphology and the Formation of Efficient Inverted Polymer Solar Cells*. Adv. Mater. 21 (14-15) (2009) 1434-1449. Available: https://doi.org/10.1002/adma.200802854.

[35] D. Demus, J.W. Goodby, G.W. Gray, H.W. Spiess, V. Vill, *Handbook of liquid crystals, volume 2A: low molecular weight liquid crystals I: calamitic liquid crystals*, John Wiley & Sons2011.

[36] M. Dridi, A. Vial. *Modeling of metallic nanostructures embedded in liquid crystals: application to the tuning of their plasmon resonance*. Opt. Lett. 34 (17) (2009) 2652-2654. Available: https://doi.org/10.1364/OL.34.002652.

[37] H. Wang, A. Vial. *Tunability of LSPR using gold nano-particles embedded in a liquid crystal cell*. J. Quant. Spectrosc. Radiat. Transf. 146 (2014) 492-498. Available: https://doi.org/10.1016/j.jqsrt.2014.02.008.

[38] N.F.F. Areed, M. El-Baz, A.M. Heikal, S.S.A. Obayya. *Intensity modulation lens on the basis of nano-scale golden rods and liquid crystal layer*. Opt. Quantum Electron. 50 (6) (2018) 240. Available: https://doi.org/10.1007/s11082-018-1501-5.

[39] Available: www.refractiveindex.info.

[40] S. Kirchmeyer, K. Reuter. *Scientific importance, properties and growing applications of poly(3,4-ethylenedioxythiophene)*. J. Mater. Chem. 15 (21) (2005) 2077-2088. Available: https://doi.org/10.1039/B417803N.

[41] A.M. Nardes, M. Kemerink, R.A.J. Janssen, J.A.M. Bastiaansen, N.M.M. Kiggen, B.M.W. Langeveld, A.J.J.M. van Breemen, M.M. de Kok. *Microscopic Understanding of the Anisotropic Conductivity of PEDOT:PSS Thin Films*. Adv. Mater. 19 (9) (2007) 1196-1200. Available: https://doi.org/10.1002/adma.200602575.

[42] B. Boroomand Nasab, A. Kosarian, N. Alaei Sheini. *Effect Of Zinc Oxide RF Sputtering Pressure on the Structural and Optical Properties of ZnO/PEDOT: PSS Inorganic/Organic Heterojunction*. Journal of Optoelectronical Nanostructures. 4 (3) (2019) 33-46. Available: https://jopn.marvdasht.iau.ir/article_3618.html.

[43] Y.Y. Kee, S.S. Tan, T.K. Yong, C.H. Nee, S.S. Yap, T.Y. Tou, G. Sáfrán, Z.E. Horváth, J.P. Moscatello, Y.K. Yap. *Low-temperature synthesis of indium tin oxide nanowires as the transparent electrodes for organic light emitting devices*. J. Nanotechnol. 23 (2) (2012) 025706. Available: https://doi.org/10.1088/0957-4484/23/2/025706.

[44] F. Assous, P. Degond, E. Heintze, P.A. Raviart, J. Segre. *On a Finite-Element Method for Solving the Three-Dimensional Maxwell Equations*. J. Comput. Phys. 109 (2) (1993) 222-237. Available: https://doi.org/10.1006/jcph.1993.1214.

[45] M.H. Muhammad, M.F.O. Hameed, S.S.A. Obayya. *Broadband absorption enhancement in periodic structure plasmonic solar cell*. Opt. Quantum Electron. 47 (6) (2015) 1487-1494. Available: https://doi.org/10.1007/s11082-015-0127-0.

[46] G. Singh, S.S. Verma. *Enhanced efficiency of thin film GaAs solar cells with plasmonic metal nanoparticles*. Energy Sources A: Recovery Util. Environ. Eff. 40 (2) (2018) 155-162. Available: https://doi.org/10.1080/15567036.2017.1407840.

[47] F.L. Teixeira. *Time-Domain Finite-Difference and Finite-Element Methods for Maxwell Equations in Complex Media*. IEEE Trans. Antennas Propag. 56 (8) (2008) 2150-2166. Available: https://doi.org/10.1109/TAP.2008.926767.

[48] M. Rezvani, M. Fathi Sepahvand. *Simulation of surface plasmon excitation in a plasmonic nano-wire using surface integral equations*. Journal of Optoelectronical Nanostructures. 1 (1) (2016) 51-64. Avalable: https://jopn.marvdasht.iau.ir/article_1815.html.

[49] B. Petter Jelle, C. Breivik, H. Drolsum Røkenes. *Building integrated photovoltaic products: A state-of-the-art review and future research opportunities*. Sol. Energy Mater. 100 (2012) 69-96. Available: https://doi.org/10.1016/j.solmat.2011.12.016.

[50] L. Beilina, V. Ruas. *Explicit P_1 Finite Element Solution of the Maxwell-Wave Equation Coupling Problem with Absorbing.* b. c. Mathematics. 12 (2024) 936. Available: https://doi.org/10.3390/math12070936.

[51] Z.C. Holman, A. Descoeudres, L. Barraud, F.Z. Fernandez, J.P. Seif, S.D. Wolf, C. Ballif. *Current Losses at the Front of Silicon Heterojunction Solar Cells*. IEEE J. Photovolt. 2 (1) (2012) 7-15. Available: https://doi.org/10.1109/JPHOTOV.2011.2174967.

[52] J. Poortmans, V. Arkhipov, *Thin film solar cells: fabrication, characterization and applications*, John Wiley & Sons2006.

[53] G. Zheng, L. Xu, M. Lai, Y. Chen, Y. Liu, X. Li. *Enhancement of optical absorption in amorphous silicon thin film solar cells with periodical nanorods to increase optical path length*. Opt. Commun. 285 (10) (2012) 2755-2759. Available: https://doi.org/10.1016/j.optcom.2012.01.084.

[54] M. Chen, Y. Cui, Y. Zhang, T. Ji, Y. Hao, F.R. Zhu. *Effect of spherical metallic nanoparticles in active layer on absorption enhancement in organic solar cells*. J. Photonics Energy. 7 (4) (2017) 045501.

[55] N. Sahraei, S. Venkataraj, A.G. Aberle, I.M. Peters. *Investigation of the Optical Absorption of a-Si:H Solar Cells on Micro- and Nano-Textured Surfaces*. Energy Procedia. 33 (2013) 166-172. Available: https://doi.org/10.1016/j.egypro.2013.05.054.

[56] D.V. Prashant, D.P. Samajdar, D. Sharma. *Optical simulation and geometrical optimization of P3HT/GaAs nanowire hybrid solar cells for maximal photocurrent generation via enhanced light absorption*. J. Sol. Energy. 194 (2019) 848-855. Available: https://doi.org/10.1016/j.solener.2019.11.027.

[57] T. Ahmed, M. K. Das. *Enhanced Efficiency in Thin Film Solar Cells: Optimized Design With Front Nanotextured and Rear Nanowire-Based Light Trapping Structur*. IEEE Transactions on Nanotechnology. 23 (2024) 456-466. Available https://doi: 10.1109/TNANO.2024.3408253.